ADVANCED FUNCTIONAL MATERIALS
www.afm-journal.de

Nano-Imprinted Ferroelectric Polymer Nanodot Arrays for High Density Data Storage

*Xiang-Zhong Chen, Qian Li, Xin Chen, Xu Guo, Hai-Xiong Ge, Yun Liu, and Qun-Dong Shen**

Ferroelectric vinylidene fluoride-trifluoroethylene copolymer [P(VDF-TrFE)] free-standing ultrahigh density (≈75 Gb inch^{-2}) nanodot arrays are successfully fabricated through a facile, high-throughput, and cost-effective nanoimprinting method using disposable anodic aluminum oxide with orderly arranged nanometer-scale pores as molds. The nanodots show a large-area smooth surface morphology, and the piezoresponse in each nanodot is strong and uniform. The preferred orientation of the copolymer chains in the nanodot arrays is favorable for polarization switching of single nanodots. The ferroelectric polymer memory prototype can be operated by a few volts with high writing/erasing speed, which comply with the requirements of integrated circuit. This approach provides a way of directly writing nanometer electronic features in two dimensions by piezoresponse force microscopy probe based technology, which is attractive for high density data storage.

1. Introduction

With the development of modern electronics, more and more organic electronic devices, such as flexible display screens and disposable radio-frequency identification (RFID) tags, come into view. The tendency of these electronic devices is miniaturization, high portability, and low-power consuming. It requires the key components, i.e., memory parts, to satisfy high density storage, low volume, light weight, fast switching speed, and long-term stability. To fulfill different needs of data storage, dynamic random access memory (DRAM), hard-disk drives (HDD), and flash memory have been used. Nevertheless, neither of them is suitable for the newly developed devices because DRAM needs refresh cycles (and thus extra power supply), HDD is too slow to access and power-consuming, and the flash has limited endurance.[1] Ferroelectric thin-film memories have been fabricated onto standard silicon integrated circuits, and take the advantages of fast switching, low power consumption, and long durability over competing nonvolatile memories.[2] Most of the ferroelectrics currently in use are inorganic materials with complex structures, which make them easily damaged in the existing lithographic process.[3] The inorganic materials are also brittle and generally fracture at low strain, and thereby are not fully compatible with the state-of-art flexible organic electronics.

As canonical organic ferroelectric materials, poly(vinylidene fluoride) (PVDF) and its copolymers, have been extensively studied for high-k composites,[4–6] electromechanical actuators,[7] ultrahigh energy density capacitors,[8,9] and on-chip cooling devices.[10] Vinylidene fluoride-trifluoroethylene copolymers, i.e., P(VDF-TrFE)s, have remnant polarization as high as 10 μC cm^{-2},[11] and show promise as materials for thin-film and non-volatile memories. Moreover, the excellent solubility, processibility, and flexibility facilitate the integration of the copolymers in electronic devices. P(VDF-TrFE)s require relatively large electric field (≈50 MV m^{-1}), usually an order of magnitude higher than those of inorganic materials, to switch the spontaneous polarization in the crystals.[11] By scaling down the film thickness to the submicrometer scale, the ferroelectric polymer memories can store data by applying bias of a few volts, which comply with the requirements of integrated circuit. Recent experimental results demonstrate that ferroelectricity persists in the copolymer thin films with thickness down to a few molecular monolayers.[12]

To achieve ultrahigh density information storage, atomic force microscopy (AFM) has been extensively used for nanoscopic write operations on continuous ferroelectric films, where the polarization of ferroelectric domains can be switched by applying a voltage between a metallic AFM tip and the bottom electrode.[13] Such nanoscale writing could produce an array of ferroelectric domains at a density of tens of gigabytes per square inch, and allow creating complicated patterns under computer control of tip motion. However, direct polarizing by the AFM tip has some drawbacks such as domain merging or collapsing due to large local field, and cross-talk where the

X. Z. Chen, X. Chen, Prof. Q. D. Shen
Department of Polymer Science & Engineering
and Key Laboratory of Mesoscopic Chemistry of MOE
School of Chemistry & Chemical Engineering
Nanjing University
Nanjing, 210093, China
E-mail: qdshen@nju.edu.cn
Q. Li, Prof. Y. Liu
Research School of Chemistry
Australian National University
ACT 0200, Australia
X. Guo, Prof. H. X. Ge
Department of Materials Science & Engineering
and National Laboratory of Solid State Microstructures
Nanjing University
Nanjing, 210093, China

DOI: 10.1002/adfm.201203042

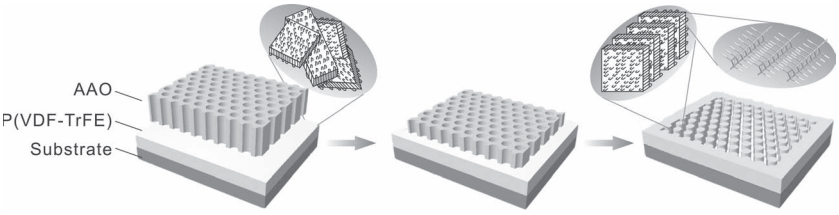

Scheme 1. Procedure of nano-imprinting P(VDF-TrFE) film with AAO as a template. The scheme also indicates preferred molecular orientation after nano-imprinting.

switching can propagate out of the target nano-domain through the continuous ferroelectric films.[14,15] An alternative way to realize ultrahigh density memory devices is nanometer-scale imprinting lithography, which allows a marked reduction in the size of data-storage elements and turns continuous film into isolated nanoscale ferroelectrics (memory units).[16–18] Thermal nano-imprinting is a high-throughput method for fabrication of large-scale regular array of polymers, and can reach a resolution as high as 5 nm. It can also be used to control the structures and physical properties of the polymers.[19–22] Nevertheless, the fabrication of nano-imprinting molds is usually rather expensive and painstaking.

In this paper, we demonstrate a facile and cost-effective method of imprinting ferroelectric polymer P(VDF-TrFE) by using disposable anodic aluminum oxide (AAO) mold with orderly arranged nanometer-scale pores. In addition to very low price, well-defined pore sizes, and narrow pore size distributions, the AAO molds have large tunability; that is, the pore diameter, center-to-center pore distance, and the packing of pores can be easily controlled by altering the AAO fabrication conditions.[23–27] The molds can be easily removed after thermal imprinting to leave free-standing ferroelectric polymer nanodot arrays. An unpredictable but interesting question is whether the ferroelectric polymers crystallize in a confined space of nanopores during imprinting process will preserve the same crystal structure and ferroelectricity as the continuous films.

2. Results and Discussion

The ferroelectric nanodot arrays are fabricated through a standard thermal imprinting lithograph technique using an AAO mold with orderly arranged nanopores (**Scheme 1**). The average pore diameter of the mold is about 70 nm, the distance between two neighboring pores is about 100 nm, and pore depth is 300 nm, as is shown in **Figure 1**a. The mold with nanopores is pressed into a 200 nm-thick P(VDF-TrFE) film spin-coated on the metalized silicon wafer. The nanostructures on the AAO mold are duplicated in a large area of the ferroelectric polymer thin film. Figure 1b shows a representative scanning electron micrograph of imprinted P(VDF-TrFE) nanodots after removal of the AAO mold. The inset in Figure 1b is a top-view of the hexagonally ordered nanodot array on the substrate. The period of the nanodot array is 100 nm, which is consistent with the period of the AAO mold. Overall, the array lacks a perfect long range translational periodicity. A comparison of the diameters of the AAO nanopores and the nanodots (≈80 nm) indicates that the compressed copolymer undergoes a lateral expansion in dimension when the mold is removed. When the P(VDF-TrFE) film is formed during spin-coating, the solvent evaporates so fast that the polymer chains are not allowed to fully adjust themselves to optimized molecular conformations, and thereby there is an internal stress residual in the film.[28] Afterwards the AAO mold is pressed into the copolymer film, and the pressure squeezes the polymer chains into the nanopores, which exerts another stress on the polymer film. All of these stresses can be released with removing the AAO mold. Therefore, the relaxation of the polymer chains leads to expansion of the nanodots.

The morphological difference and ferroelectric properties of P(VDF-TrFE) continuous thin film and imprinted nanodots are investigated by piezoresponse force microscopy. **Figure 2** shows the topographic, piezoresponse force microscopy (PFM) amplitude, and PFM phase images obtained simultaneously for the same area (1 μm × 1 μm) of the annealed P(VDF-TrFE) films and the copolymer nanodot arrays. In a topographic image, P(VDF-TrFE) continuous film obtained by thermal annealing on the substrate shows rough surface with many ridges on its

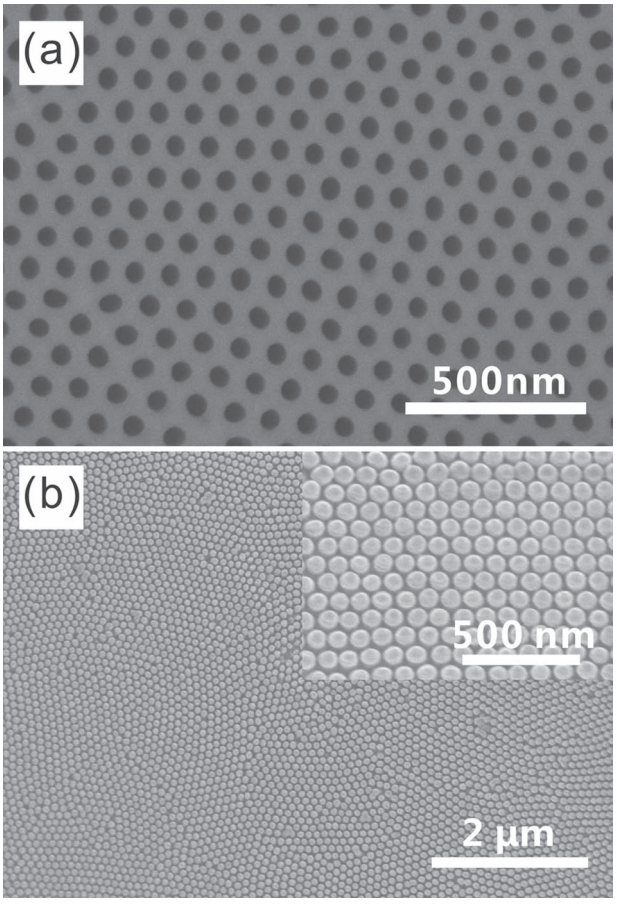

Figure 1. SEM images of a) the AAO mold and b) large scale ferroelectric P(VDF-TrFE) nanodot arrays fabricated by the nano-imprinting method. The inset of (b) shows a magnified image of the nanodot arrays.

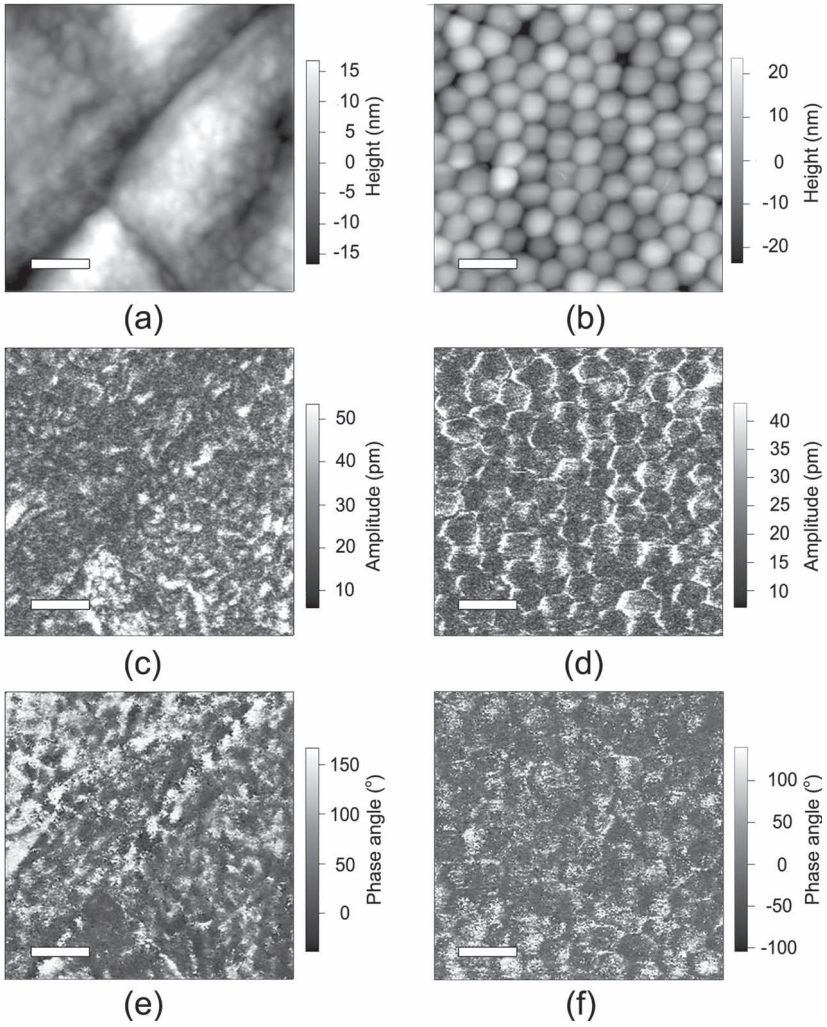

Figure 2. a,b) Topographic, and the corresponding c,d) PFM amplitude and e,f) PFM phase images for the annealed P(VDF-TrFE) films (left column) and the P(VDF-TrFE) nanodot arrays (right column). All the scale bars in the images are 200 nm.

surface (see Figure S1 in the Supporting Information). The ridges on the wrinkled film come from packing of folded chain during the crystallization, as a result of the mismatch of surface energy between the substrate and P(VDF-TrFE) film.[29] As can be seen in Figure 2a, besides large height difference between the ridges and valley, the annealed film exhibits lots of small grains with size of tens of nanometers randomly packing together. By contrast, the nanodots show a large-area smooth surface morphology (Figure 2b). This indicates that the crystallization becomes uniform when the copolymer chains are pressed into a confined space.

The piezoresponse amplitude images and phase images are presented in Figure 2c–f. The amplitude image for the P(VDF-TrFE) continuous films consist of bright regions with irregular shapes and strong piezoelectric response, which is randomly distributed in dark (unpolarized) regions (Figure 2c). Apparently, the PFM amplitude image does not coincide well with the topography image (Figure 2a), indicating that those crystallite grains may not necessarily be single domains. In contrast, all P(VDF-TrFE) nanodots are distinguished as dark regions, which is outlined by bright narrow regions (Figure 2d). The brighter regions (higher piezoresponse) around the nanodot boundaries may result from a better chain alignment in the material, as described elsewhere.[22]

PFM phase images directly reflect the information of polarization orientations. Anti-parallel domains have 180° phase difference, and in our case, the phase for those domains with downward polarization is adjusted around 0°. No well-defined domain pattern can be observed in the annealed P(VDF-TrFE) (Figure 2e). The phase angles randomly distribute among 0° and 180°, indicating the disordered orientation of polarization in the continuous copolymer films. On the other hand, the piezoresponse in each nanodot is rather uniform, and a majority of the polymer nanodots have a phase of about 0° (Figure 2f), suggesting enhanced alignment of dipoles along the polymer chains and good uniformity of polymer crystallites. The regions of uniform polarization correspond well to the topographic structure.

To further investigate the polarization switching characteristics of the P(VDF-TrFE), piezoresponse hysteresis loops are acquired at random locations of the continuous film or near the center of the nanodots. Typical loops are shown in **Figure 3**a. Both the continuous film and the nanodots exhibit polarization reversibility; i.e., the polarization directions can be switched at both polarities of tip voltages. Both piezoresponse loops are horizontal shifted slightly, which may be caused by an internal bias field inside the materials[30,31] and/or work function difference between the top electrode (Pt-coated silicon probe) and the bottom electrode (gold). The apparent coercive field of the continuous film is about 85 MV m^{-1}, which is larger than the corresponding that of bulk copolymer (50 MV m^{-1}). One possible reason is that interface misfit of the copolymer and gold substrate changes the ferroelectric switching behavior when the film thickness is scaled down to the nanometer scale.[32–34] Another important fact is that in PFM measurements, the switching bias field is applied via a sharp tip, and thus the field is inhomogeneous as opposed to conventional ferroelectric tests. Nanodot has a lower coercive field than the continuous film (≈65 MV/m), as estimated from its coercive voltage and thickness (175-nm-high dot plus 30 nm residual film). For the nanodots crystallized in a confined space, copolymer chains may experience less entanglement with those from adjacent nanodots, which may favor the polarization switching of single nanodots.[20]

Field-induced nanometer-scale displacement behavior in the P(VDF-TrFE) thin film and nanodots are also studied by PFM. The presence of the ferroelectric domain structures is further

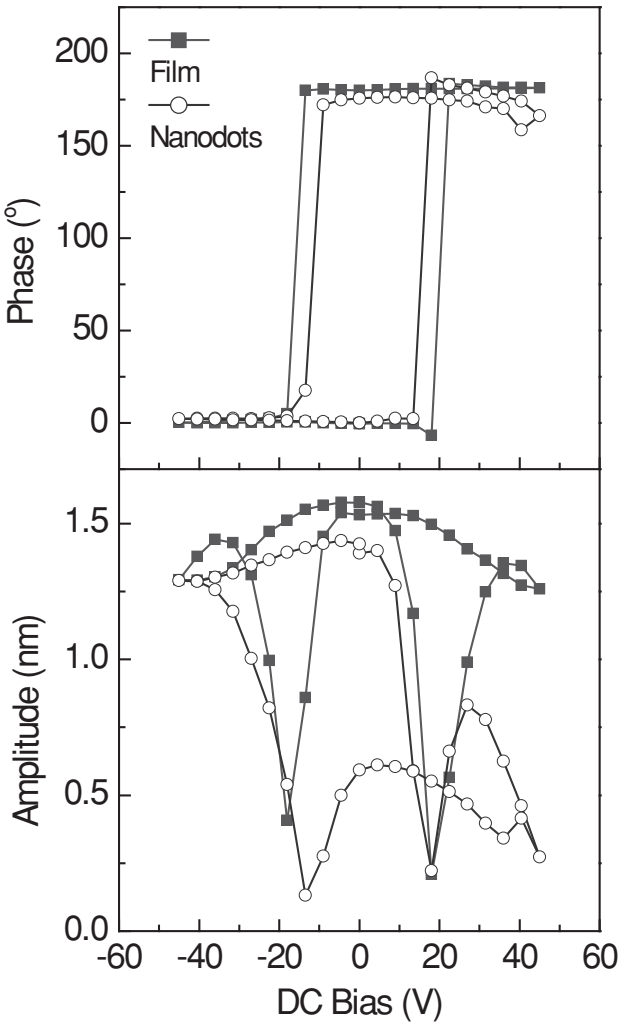

Figure 3. Piezoresponse a) phase and b) amplitude loops obtained from the P(VDF-TrFE) continuous film and nanodots.

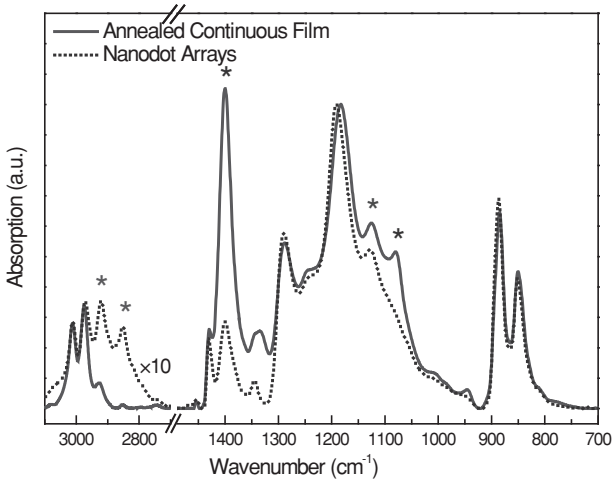

Figure 4. Infrared spectra of the annealed continuous film and imprinted nanodots.

confirmed by the amplitude loops (Figure 3b), which exhibit butterfly-type shape characteristic of a ferroelectric material. For the nanodots, an asymmetric piezoelectric behavior is observed and may be attributed to interface effects or preferred orientation of the dipoles in the nanodots.[35]

Reflection-absorption infrared spectra of the imprinted P(VDF-TrFE) nanodot arrays and the annealed continuous film are shown in **Figure 4**, which is used to measure localized chain conformation, packing, and orientation. The vibrational bands for the copolymers at 1290 and 850 cm^{-1} have been assigned to specific conformations, i.e., $T_m \geq_4$ (trans isomer sequences four or more units long) and $T_m \geq_3$, respectively.[11] These bands are therefore characteristic of the ferroelectric phase in both samples.

The bands in a range of 1500–800 and 3100–2700 cm^{-1} show the most interesting structural differences between two copolymer samples. The 1400 and 1080 cm^{-1} bands belong to the CH_2 wagging vibration with the dipole moment along the chain direction (c axis).[36] For copolymer nanodot arrays, the intensities of these bands are rather weak, which indicates that the planar zigzag polymer chains are aligned parallel to the substrate. In contrast, the annealed continuous film shows the strong absorption bands at 1400 and 1080 cm^{-1}, suggesting the copolymer chains are aligned tilted or normal to the substrate. The nanodot arrays show strong absorption band at 2920 and 2850 cm^{-1}. These bands are assigned to the CH_2 asymmetric and symmetric stretching[35] with the dipole moments parallel to the b axis, and perpendicular to the polymer chain direction. Thus b axis is perpendicular to the substrate. The preferred orientation of the copolymer chains in the nanodot arrays is favorable for rotation of dipoles on application of an electric field vertical to the substrate in the PFM measurement.

The band at 1290 cm^{-1} has been assigned to crystalline phase and does not overlap with any disorder phase band.[36] The shoulder band at 1240 cm^{-1} is associated with amorphous phase. And the absorption band at 1182 cm^{-1} is crystallinity-insensitive, and can be chosen as internal standard to clarify the contribution of order and disorder phases. It is obvious that there are no significant differences between the annealed film and the nanodot arrays.

PFM-probe based technology has the potential to achieve ultrahigh density and high rate data storage using ferroelectric materials. The writing and reading on the imprinted copolymer nanodot array are examined. The writing is realized by applying a DC voltage between a metalized PFM tip and the substrate as the tip scanned over the surface of the copolymer, which leads to polarization of the ferroelectric domains. Then the reading is carried out by monitoring the piezoelectric vibration of the polarized area of ferroelectric polymer film under AC voltage. The PFM phase image of the copolymer nanodot arrays after writing a capital letter "A" with a positive bias is shown in **Figure 5**a, where the background is uniformly polarized with a negative voltage before writing. It is evident that the letter appears as bright area with phase angle quite different with that of the unwritten area. Therefore, upward or downward polarization state can be denoted as "1" or "0", corresponding with the well-established binary memory system. The information

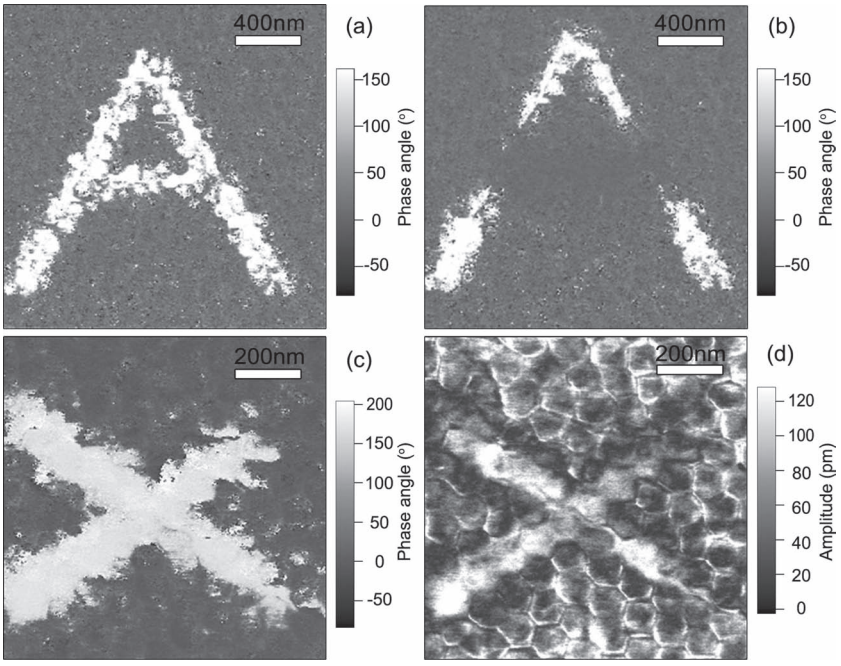

Figure 5. Demonstration of data memory on the nanoimprinted VDF-TrFE copolymers. a,b) PFM phase images show that the letter "A" written on the nanodot arrays and then erased by applying a field. c,d) PFM phase and amplitude images show that the letter "X" written by applying a positive electric field.

recorded on the copolymer nanodot arrays can also be erased by applying a negative DC voltage in an interesting area. As shown in Figure 5b, the cross in letter "A" disappeared after erasing operation. The "write-erase" procedure is completely reversible, making it applicable for data storage.

Figure 5c,d show high resolution PFM phase and amplitude images of the written area. Each line of "X" occupies only one line of nanodot arrays. For comparison, the written image on nano-imprinted copolymer film with one-dimensional pattern (vertically aligned 200nm-period gratings) is also investigated (Figure S2 in the Supporting Information). It is noteworthy that the written area with an acronym "EAP", shorting for "electroactive polymers", tends to spread along the trench, regardless of the heading direction of PFM tip. It appears that polarizing switching by the PFM tip can propagate out of the target nanodomain through the continuous ferroelectric films. In contrast, the nanodots switch independently of each other, and thus can effectively prevent domain merging or cross-talk. Assuming the ferroelectric nanodots (memory units) are arranged hexagonally, the data storage density is estimated to achieve a value of as high as 75 Gb inch^{-2}.

3. Conclusions

Ferroelectric polymer film with ultrahigh nanodot density has been successfully fabricated through a facile, high-throughput (in half an hour instead of half-day annealing in the case of continuous films), and cost-effective method of imprinting by using disposable anodic aluminum oxide mold with orderly arranged nanometer-scale pores, followed by removal of the mold to leave free-standing nanodot arrays. The nanodots show a large-area smooth surface morphology, and the piezoresponse in each nanodot is strong and uniform. The preferred orientation of the copolymer chains, which are aligned parallel to the substrate, in the nanodot arrays is favorable for polarization switching of single nanodots. This approach allows nanometer electronic feature to be written directly in two dimensions by PFM-probe based technology, and can reach a resolution in the order of <10 nm. Thus the data storage density of ferroelectric copolymer nanodot arrays can achieve tens or hundreds Gb inch^{-2}. The ferroelectric polymer arrays can be operated by a few volts with high writing/erasing speed, which comply with the requirements of integrated circuit.

4. Experimental Section

Materials: P(VDF-TrFE) (68/32 mol/mol) was purchased from Solvay. Other reagents were used as received.

Preparation of Highly Ordered AAO Mold: High purity (99.999%) aluminum foils with the thickness of 150 μm were employed for the anodization. After careful cleaning and annealing, the aluminum foils were anodized for the first time under constant potentials of 40–60 V in 0.3 M oxalic acid. Second-time anodizations were employed under same potentials in order to obtain 300 nm pore depth.[37] The pore diameter was adjusted by immersing the PAA samples into 5 wt% phosphoric acid at 30 °C. The precise control of both electrolyte and phosphoric acid temperatures was achieved by a homebuilt external-cycling setup with JULABO F12-ED cooling system (–20 to 100 °C), which is very important for adjusting PAA thickness and pore diameter.

Thin Film Preparation: A 15-nm-thick gold layer was deposited together with a 5 nm chromium adhesion layer by means of thermal evaporation on a silicon wafer for bottom electrode use. P(VDF-TrFE) was dissolved in methyl ethyl ketone to form a uniform solution with a concentration of 2% (w/v). Next the solution was dropped on the metalized silicon wafer and then spin coated at 3000 rpm. The thin film obtained was about 200-nm thick.

Nanostructure Fabrication: The nanoimprint experiments were carried out with Wuxi ImprintNano YPL-NIL-SI400 Nanoimprint Facilities. The spin-coated film was put under the AAO mold, on which a poly(dimethylsiloxane) (PDMS) cushion was placed as a buffer layer. A pressure of 0.5 MPa was applied to the stacked system at 135 °C and was held for 10 min to partially relax the stress induced by flow and increase the crystallinity. The pressure was held until the system was cooled to room temperature. Then the patterned films to which the AAO mold stuck were carefully floated over a solution of $CuCl_2$/HCl mixture to chemically etch the aluminum foil, followed by immersing in H_3PO_4 solution (5 wt%) for 30 min to completely remove the AAO mold. Then the ferroelectric polymer nanodot arrays were rinsed with deionized water and dried in an oven prior to characterizations.

Characterization: Infrared absorption spectra for VDF-TrFE copolymer films were obtained at room temperature on an iS10 spectrometer equipped a SMART-iTR accessory with diamond crystal at 4 cm^{-1} resolution. Images of nanodot arrays and AAO mold were acquired by Hitachi S-4800 FE-SEM.

Piezoresponse force microscopy (PFM) investigations were performed on a commercial atomic force microscope (Cypher AFM, Asylum Research) under ambient conditions. Two types of Pt-coated Si probes,

i.e., Olympus AC240TM (spring constant $k \approx 2$ N m^{-1}) and Nanosensor PPP-CONTPt ($k \approx 0.2$ N m^{-1}), were used, and the imaging contact force set-points were carefully controlled around 10 nN. For domain imaging, we used off contact-resonance ac signals (typically 10 kHz, amplitude $V_{AC} = 1$–5 V) to excite the surface oscillations. To acquire local PR (piezoresponse) loops, dual ac signals ($V_{AC} = 1$ V, near 280 kHz for AC240TM probes) were superimposed on a 0.5 Hz triangular staircase wave based on the DART (dual ac resonance tracking) technique. Both the writing time and reading time were 25 ms, and only the remnant-state data were presented. Local poling tests were realized by dragging the tips at interested areas with bias voltages applied according a pre-defined pattern.

Supporting Information

Supporting Information is available from the Wiley Online Library or from the author.

Acknowledgements

This work is supported by National Natural Science Foundation of China (No. 21274057), Fundamental Research Funds for the Central Universities (No. 1103020504), and Scientific Research Foundation of Graduate School of Nanjing University (No. 2010CL06).

Received: October 18, 2012
Revised: December 17, 2012
Published online: January 17, 2013

[1] J. C. Scott, L. D. Bozano, *Adv. Mater.* **2007**, *19*, 1452.
[2] J. F. Scott, *Science* **2007**, *315*, 954.
[3] W. Lee, H. Han, A. Lotnyk, M. A. Schubert, S. Senz, M. Alexe, D. Hesse, S. Baik, U. Gosele, *Nat. Nanotechnol.* **2008**, *3*, 402.
[4] Q. M. Zhang, H. F. Li, M. Poh, F. Xia, Z. Y. Cheng, H. S. Xu, C. Huang, *Nature* **2002**, *419*, 284.
[5] J. W. Wang, Q. D. Shen, C. Z. Yang, Q. M. Zhang, *Macromolecules* **2004**, *37*, 2294.
[6] C. C. Wang, J. F. Song, H. M. Bao, Q. D. Shen, C. Z. Yang, *Adv. Funct. Mater.* **2008**, *18*, 1299.
[7] Q. M. Zhang, V. Bharti, X. Zhao, *Science* **1998**, *280*, 2101.
[8] B. J. Chu, X. Zhou, K. L. Ren, B. Neese, M. R. Lin, Q. Wang, F. Bauer, Q. M. Zhang, *Science* **2006**, *313*, 334.
[9] X. Z. Chen, Z. W. Li, Z. X. Cheng, J. Z. Zhang, Q. D. Shen, H. X. Ge, H. T. Li, *Macromol. Rapid Commun.* **2011**, *32*, 94.
[10] B. Neese, B. J. Chu, S. G. Lu, Y. Wang, E. Furman, Q. M. Zhang, *Science* **2008**, *321*, 821.
[11] H. S. Nalwa, *Ferroelectric Polymers: Chemistry, Physics, and Applications*, Marcel Dekker, New York **1995**.
[12] A. V. Bune, V. M. Fridkin, S. Ducharme, L. M. Blinov, S. P. Palto, A. V. Sorokin, S. G. Yudin, A. Zlatkin, *Nature* **1998**, *391*, 874.
[13] S. V. Kalinin, A. Gruverman, Eds., *Scanning Probe Microscopy: Electrical and Electromechanical Phenomena at the Nanoscale*, Springer, New York **2007**.
[14] D. A. Bonnell, S. V. Kalinin, A. L. Kholkin, A. Gruverman, *MRS Bull.* **2009**, *34*, 648.
[15] H. Han, Y. Kim, M. Alexe, D. Hesse, W. Lee, *Adv. Mater.* **2011**, *23*, 4599.
[16] S. Y. Chou, P. R. Krauss, P. J. Renstrom, *Appl. Phys. Lett.* **1995**, *67*, 3114.
[17] M. D. Austin, H. X. Ge, W. Wu, M. T. Li, Z. N. Yu, D. Wasserman, S. A. Lyon, S. Y. Chou, *Appl. Phys. Lett.* **2004**, *84*, 5299.
[18] Z. W. Li, Y. N. Gu, L. Wang, H. X. Ge, W. Wu, Q. F. Xia, C. S. Yuan, Y. Chen, B. Cui, R. S. Williams, *Nano Lett.* **2009**, *9*, 2306.
[19] M. Zhou, M. Aryal, K. Mielczarek, A. Zakhidov, W. Hu, *J. Vac. Sci. Technol. B* **2010**, *28*, C6M63.
[20] Z. J. Hu, G. Baralia, V. Bayot, J. F. Gohy, A. M. Jonas, *Nano Lett.* **2005**, *5*, 1738.
[21] Z. J. Hu, M. W. Tian, B. Nysten, A. M. Jonas, *Nat. Mater.* **2009**, *8*, 62.
[22] Y. M. Liu, D. N. Weiss, J. Y. Li, *ACS Nano* **2010**, *4*, 83.
[23] S. Z. Chu, K. Wada, S. Inoue, M. Isogai, A. Yasumori, *Adv. Mater.* **2005**, *17*, 2115.
[24] O. Jessensky, F. Muller, U. Gosele, *Appl. Phys. Lett.* **1998**, *72*, 1173.
[25] O. Jessensky, F. Muller, U. Gosele, *J. Electrochem. Soc.* **1998**, *145*, 3735.
[26] S. H. Chen, D. S. Chan, C. K. Chen, T. H. Chang, Y. H. Lai, C. C. Lee, *Jpn. J. Appl. Phys.* **2010**, *49*, 015201.
[27] H. Masuda, H. Asoh, M. Watanabe, K. Nishio, M. Nakao, T. Tamamura, *Adv. Mater.* **2001**, *13*, 189.
[28] K. R. Thomas, A. Chenneviere, G. Reiter, U. Steiner, *Phys. Rev. E* **2011**, *83*, 021804.
[29] D. Guo, I. Stolichnov, N. Setter, *J. Phys. Chem. B* **2011**, *115*, 13455.
[30] A. Baji, Y. W. Mai, Q. Li, Y. Liu, *Nanoscale* **2011**, *3*, 3068.
[31] Q. Li, Y. Liu, J. Schiemer, P. Smith, Z. R. Li, R. L. Withers, Z. Xu, *Appl. Phys. Lett.* **2011**, *98*, 092908.
[32] R. C. G. Naber, P. W. M. Blom, A. W. Marsman, D. M. de Leeuw, *Appl. Phys. Lett.* **2004**, *85*, 2032.
[33] H. S. Xu, J. H. Zhong, X. B. Liu, J. H. Chen, D. Shen, *Appl. Phys. Lett.* **2007**, *90*, 092903.
[34] F. Xia, H. S. Xu, F. Fang, B. Razavi, Z. Y. Cheng, Y. Lu, B. M. Xu, Q. M. Zhang, *Appl. Phys. Lett.* **2001**, *78*, 1122.
[35] K. Matsushige, H. Yamada, H. Tanaka, T. Horiuchi, X. Q. Chen, *Nanotechnology* **1998**, *9*, 208.
[36] K. J. Kim, N. M. Reynolds, S. L. Hsu, *Macromolecules* **1989**, *22*, 4395.
[37] G. Q. Ding, M. J. Zheng, W. L. Xu, W. Z. Shen, *Nanotechnology* **2005**, *16*, 1285.